ELSEVIER

The Chemical Engineering Journal 57 (1995) 155–162

THE CHEMICAL ENGINEERING JOURNAL

The Maxwell–Stefan description of mass transport across zeolite membranes

R. Krishna, L.J.P. van den Broeke

Department of Chemical Engineering, University of Amsterdam, Nieuwe Achtergracht 166, 1018 WV Amsterdam, Netherlands

Abstract

Published experimental data on transient permeation fluxes of light hydrocarbons through a silicalite-1 membrane show curious behaviour. For a mixture of methane and *n*-butane, for example, the transient experiments showed that initially the permeation flux of methane is higher than for *n*-butane but that this methane flux reduces to a lower steady state value. The *n*-butane flux is initially low but under steady state conditions is much higher than that for methane. A mathematical model for transient membrane mass transport has been developed using the Maxwell–Stefan formulation. This model is able to predict the observed maximum in the flux of methane, and if we assume that the Fick diffusivity is constant the transient permeation fluxes are predicted to reach their steady state values monotonically. Thus the Fick formulation fails even at the qualitative level to explain the experimental results.

It is concluded that the Maxwell–Stefan formulation is indispensable for the description of mass transport across zeolite membranes.

Keywords: Mass transfer; Zeolite membrane; Maxwell–Stefan theory; Fick formulation; Microporous diffusion

1. Introduction

Membrane separations are currently gaining in importance [1] and separations based on microporous membranes such as zeolites, microporous carbons and carbon molecular sieves will gain increasing attention and applications in the future [2]. Rao and Sircar [2] have shown exciting separation possibilities offered by microporous carbon membranes for separating hydrocarbons from a gaseous mixture containing hydrogen. Fig. 1 shows a typical application of hydrogen recovery from a hydrocarbon stream in a refinery. The membrane selectivity is in favour of the more strongly adsorbed hydrocarbons rather than for hydrogen which is relatively poorly adsorbed. This micropore membrane selectivity is the inverse of the usual Knudsen selectivity in favour of hydrogen when using, for example, ceramic membranes.

Recent experimental results obtained in the research group of Moulijn at the Technical University of Delft [3] illustrate the dramatic selectivity in favour of *n*-butane over hydrogen for transport through a silicalite-1 membrane (see Fig. 2). In the early stages of the transient transport process we note a high flux of hydrogen, which reduces to very low values under steady state conditions. For a silicalite-1 membrane, Kapteijn et al. [4] have recently reported selectivities in favour of the more strongly adsorbed propane in an equimolar mixture containing propane and propene (see Fig. 3). Bakker et al. [5] have also reported very interesting, and intriguing, permeation results in a zeolite membrane. An example of their experimental results is shown in Fig. 4. Fig. 4(a) shows the permeation results of single components methane (1) and *n*-butane (2). The upstream conditions are such that the partial pressures of the permeating components are $p_{10}=50$ kPa and $p_{20}=50$ kPa. The steady-state flux of methane is much larger than that of *n*-butane. Fig. 4(b) shows the experimental results obtained with an equimolar mixture of methane (1) and *n*-butane (2), each with a partial pressure of 50 kPa on the upstream side. The methane flux peaks to a maximum value before dropping to a low steady-state value. This steady-state flux of methane is much lower than that of *n*-butane. The peaking of the methane flux is analogous to the peaking of the hydrogen flux in the experiment portrayed in Fig. 2. A further interesting experimental observation of Bakker et al. [5] is shown in Fig. 4(c). Here the partial pressures of methane and *n*-butane on the upstream side are maintained at $p_{10}=95$ kPa and $p_{20}=5$ kPa. In this experiment the maximum in the methane flux increases above the value for the case where $p_{10}=50$

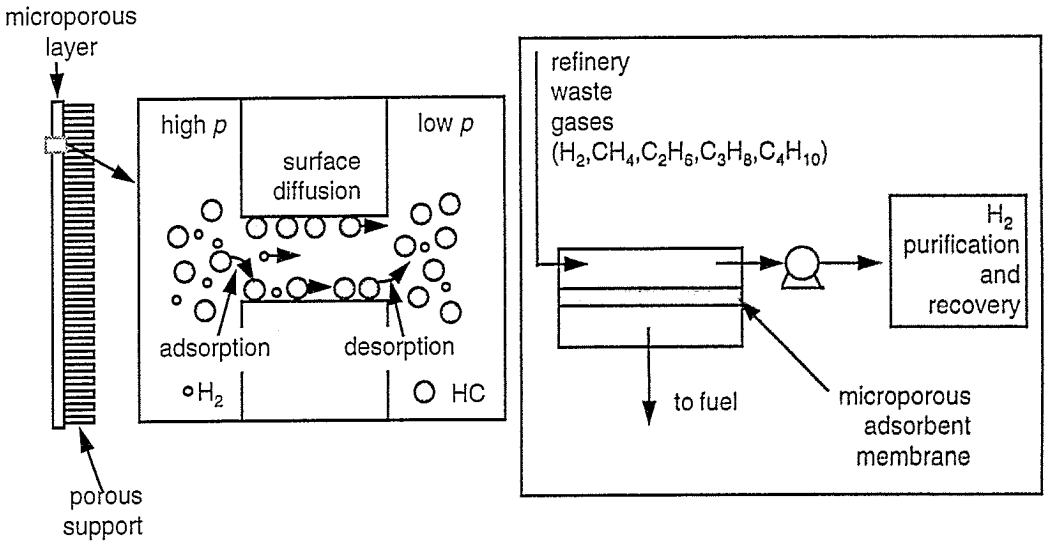

Fig. 1. A microporous carbon membrane can be used for separation of hydrocarbons from a gaseous mixture containing hydrogen. The hydrocarbons are more strongly adsorbed inside the micropores and are transported across the membrane much faster than hydrogen. Adapted from Rao and Sircar [2].

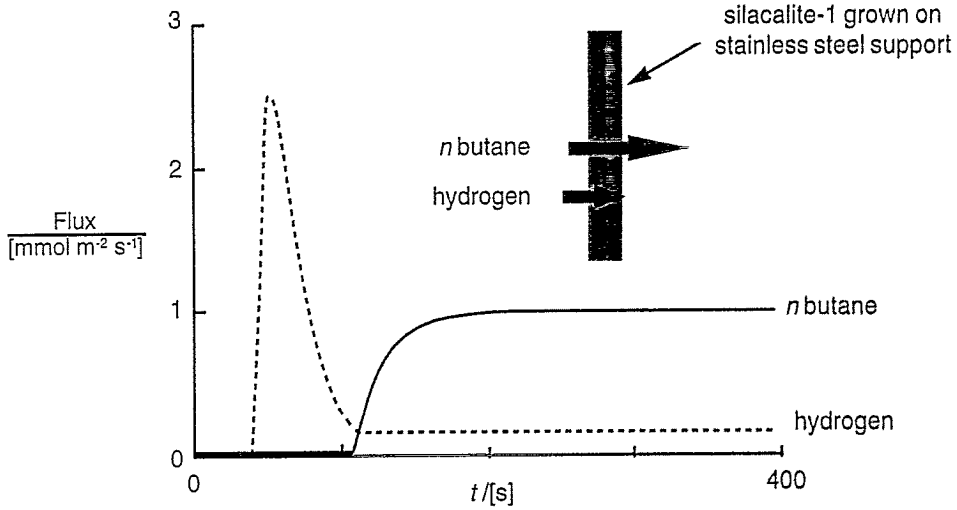

Fig. 2. Transport of *n*-butane and hydrogen across a silicalite membrane on stainless steel support; adapted from Bakker [3]. The experimental conditions were as follows, $p_{10}=50$ kPa; $p_{20}=50$ kPa. The downstream pressure was maintainted at $p_\delta=100$ kPa and a sweep gas was used. The membrane thickness was $\delta=40$ mm. The temperature was maintained at 292 K.

kPa and $p_{20}=50$ kPa. In other words the transient permeation behaviour is apparently also a function of the feed composition.

Our objective in this work is to model transient transport across microporous membranes and to demonstrate the need to adopt the Maxwell–Stefan formulation developed by Krishna [6–8].

2. Mathematical model for micropore membrane transport

Consider a membrane of thickness δ, separating two well-mixed compartments (see Fig. 5). We shall ignore the mass transfer resistances external to the membrane and consider the transfer fluxes to be determined solely by intra-(microporous)-membrane transport. At time $t=0$, a gaseous mixture is introduced into the left compartment at pressure p_0 and this composition is maintained throughout the experiment. The downstream compartment is maintained at a pressure p_δ and our interest is in the determination of the transient fluxes until steady state is reached.

The interior of the membrane is initially considered to be totally uncovered by the transferring species, i.e.

$$t=0,\ 0\leqslant z\leqslant\delta,\ \theta_{iz}=0 \tag{1}$$

At the left fluid–membrane interface we have the equilibrium relation using the extended Langmuir isotherm

$$t\geqslant 0,\ z=0;\ \theta_{i0}=\frac{b_i p_{i0}}{1+b_1p_{10}+b_2p_{20}+\ldots+b_np_{n0}} \tag{2}$$

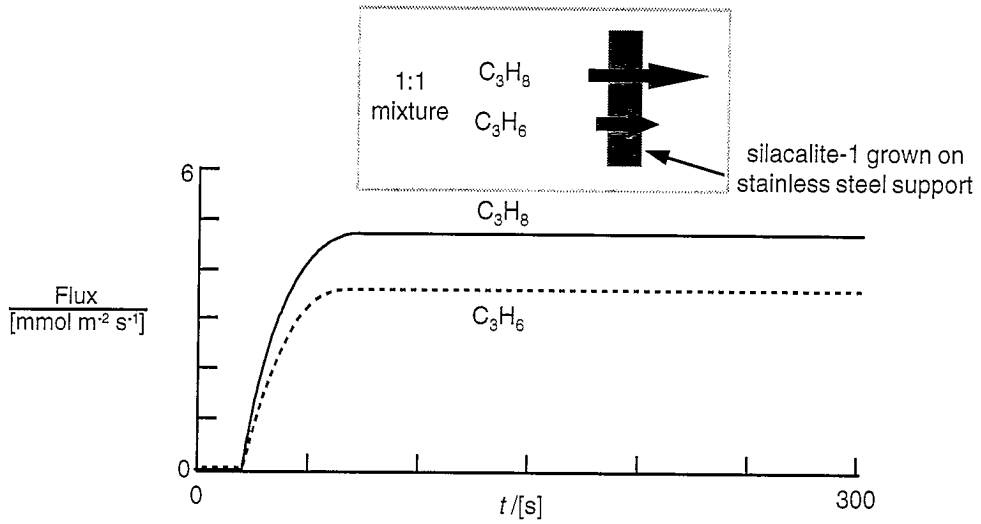

Fig. 3. Experimental results for transport of propene (1)-propane (2) across silicalite-1 membrane. Adapted from Kapteijn et al. [4]. The experimental conditions were as follows. $p_{10}=50$ kPa; $p_{20}=50$ kPa. The downstream pressure was maintainted at $p_\delta=100$ kPa and a sweep gas was used. The membrane thickness was $\delta=40$ mm. The temperature was maintained at 292 K.

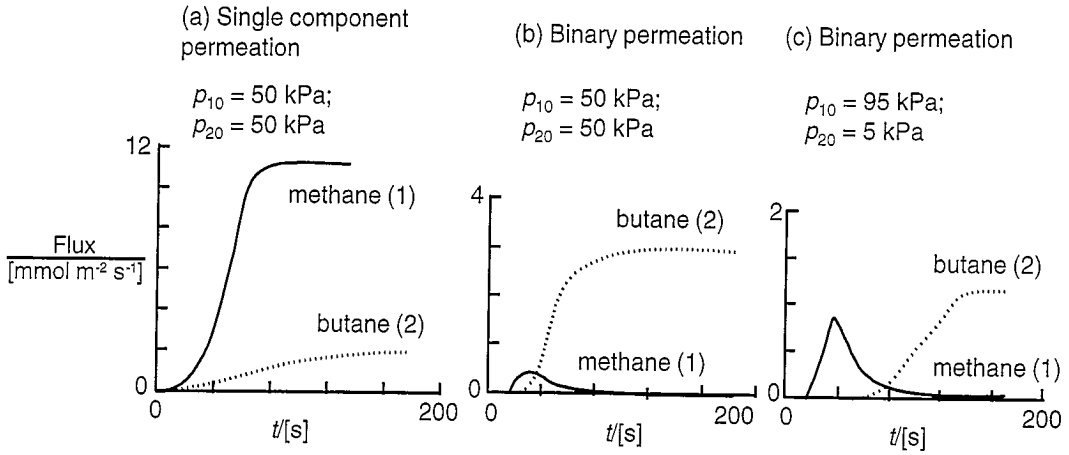

Fig. 4. Experimental results for transport of methane (1)-butane (2) across silicalite-1 membrane. Adapted from Bakker et al. [5]. The membrane thickness was $\delta=40$ mm. The temperature was maintained at 292 K.

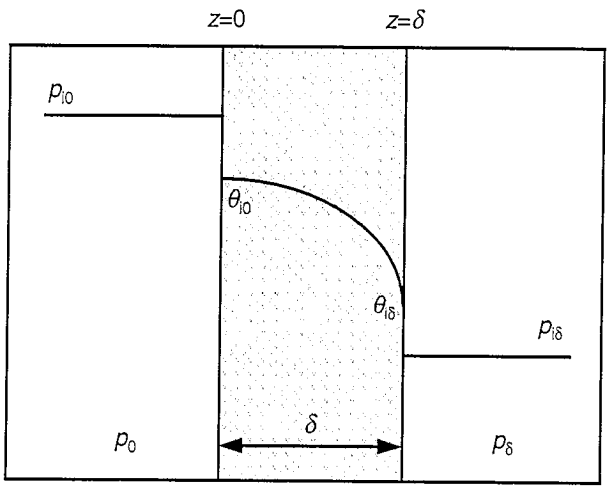

Fig. 5. Schematic of microporous membrane with two well-mixed gaseous compartments on either side.

The initial condition at the right fluid–membrane interface is

$$t=0;\ z=\delta;\ \theta_{i\delta}=0 \tag{3}$$

The differential equations describing the transient surface occupancies are

$$\frac{\partial(\theta)}{\partial t}=\frac{\partial}{\partial z}\left([D]\frac{\partial(\theta)}{\partial z}\right) \tag{4}$$

where we adopt n-dimensional matrix notation, where n represents the number of transferring species. $[D]$ is the matrix of Fick micropore diffusivities.

In order to be able to predict the Fick matrix of micropore diffusivities, we need further insight into micropore diffusion. The mechanism of transport of molecules inside micropores is by activated movement

of adsorbed species along sorption sites – this motion of sorbed species can be modeled using the Maxwell–Stefan formulation by considering the vacant sites as pseudo species, as discussed in detail by Krishna [6–8]. It follows from the Maxwell–Stefan theory that the transport fluxes can be expected to depend on (i) the Maxwell–Stefan micropore diffusivities of the transferring species, $Đ_i$, (ii) the matrix of thermodynamic factors $[\Gamma]$, which can be derived from the adsorption isotherm and (iii) the gradients of the surface occupancies inside the micropores. If we adopt the single file diffusion model for micropore diffusivities and assume the Maxwell–Stefan diffusivities $Đ_i$ to be coverage independent we have the following structure for the Fick matrix $[D]$

$$[D]=\begin{bmatrix} Đ_1 & 0 & 0 & 0 \\ 0 & Đ_2 & 0 & 0 \\ 0 & 0 & & 0 \\ 0 & 0 & 0 & Đ_n \end{bmatrix}[\Gamma] \tag{5}$$

(Maxwell–Stefan single file diffusion model)

where $[\Gamma]$, the matrix of thermodynamic factors is given by

$$\Gamma_{ij}=\delta_{ij}+\frac{\theta_i}{\theta_V}; \qquad i,j=1,2,\ldots n \tag{6}$$

In the simulations to be presented below we also consider a model in which the Fick matrix is assumed to be independent of the coverages, i.e.

$$[D]=\begin{bmatrix} Đ_1 & 0 & 0 \\ 0 & Đ_2 & 0 \\ 0 & 0 & 0 \\ 0 & 0 & Đ_n \end{bmatrix} \tag{7}$$

(constant Fick $[D]$ model)

The molar fluxes across the membrane can be calculated from

$$(N)=-\rho\epsilon q_{sat}[D]\frac{\partial(\theta)}{\partial z}\Bigg|_{z=\delta} \tag{8}$$

where the occupancy gradients can be evaluated at either $z=0$ or at $z=\delta$ because the fluxes N_i are z-invariant. In Eq. (8), q_{sat} represents the saturation concentration of adsorbed species typically expressed in mol kg^{-1} of membrane; ρ is the density of the membrane expressed in kg m^{-3}; ϵ is the membrane porosity. With diffusivities expressed in $m^2\ s^{-1}$ and the fluxes are calculated to be in the units of mol per m^2 of membrane area per second.

It is convenient to cast the differential equation in non-dimensional form by defining the Fourier number, defined in terms of a reference value for the Maxwell–Stefan diffusivity:

$$\mathrm{Fo}=\frac{Đ_{ref}t}{\delta^2} \tag{9}$$

In the simulations reported below we take $Đ_{ref}$ to be the lowest value of the Maxwell–Stefan diffusivities $Đ_i$. With this definition Eq. (4) may be recast as

$$\frac{\partial(\theta)}{\partial \mathrm{Fo}}=\frac{\partial}{\partial\eta}\left(\frac{[D]}{Đ_{ref}}\frac{\partial(\theta)}{\partial\eta}\right) \tag{10}$$

where η is the dimensionless distance

$$\eta=z/\delta \tag{11}$$

In the simulations presented below the set of coupled partial differential Eqs. (4) were solved using the method of lines [9] to calculate the dimensionless fluxes $(N_i\delta)/(\rho\epsilon q_{sat}Đ_{ref})$ as a function of the Fourier number. Such simulations are functions only of three parameters: b_1, b_2/b_1 and $Đ_1/Đ_2$.

3. Simulation results for transient fluxes across membrane

In the following section numerical simulations for three different permeation experiments are discussed.

3.1. Separation of propane/propene mixture across silicalite membrane

Using the Maxwell–Stefan diffusivities $Đ_i$ and the adsorption isotherm reported by Kapteijn et al. [4] we performed simulations for transient transport of an equimolar mixture of propene (1) and propane (2) across a silicalite-1 membrane. The results are shown in Fig. 6. The model parameters are listed in the legend to Fig. 6. Kapteijn et al. [4] do not report the downstream partial pressures of the permeating components, and in the simulations of Figs. 6–11, these are assumed to be negligibly small due to a high sweep gas rate on the downstream side. We see that the predicted transient fluxes of both components reflect the correct trends in the permeation behaviour of the system as observed experimentally; compare Figs. 3 and 6. In the paper by Kapteijn et al. [4] only a steady-state model had been presented for the Maxwell–Stefan single file diffusion; these authors concluded that the Maxwell–Stefan model is superior to the simple-minded Fick model. A further point worthy of note is that the weak maximum in the propene flux, as found in the simulations has also been detected experimentally by Kapteijn et al. [4]; cf. Figs. 3 and 6.

For the system propane/propene the adsorption strengths are close to each other. Below we analyze

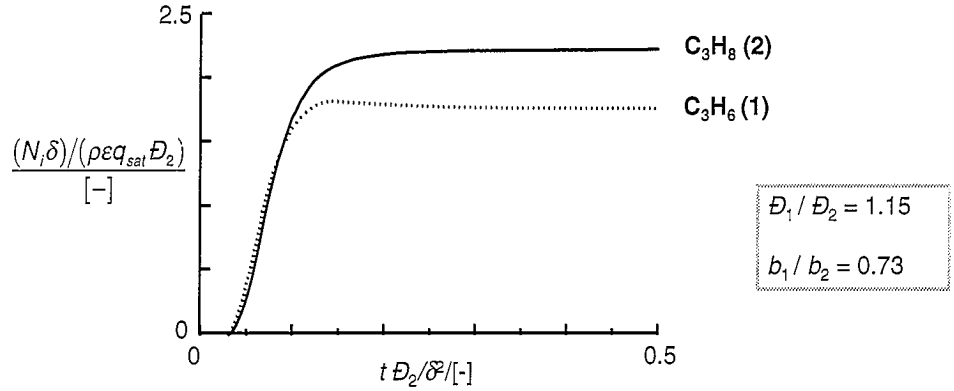

Fig. 6. Simulations for transport of propene (1)-propane (2) across silicalite membrane. Conditions reported in the legend to Fig. 3. The parameter inputs are: $b_1=0.96$ kPa^{-1}; $b_1/b_2=0.73$; $Đ_1/Đ_2=1.15$. The upstream partial pressures of the methane (1) and butane (2) are $p_{10}=$ 50 kPa; $p_{20}=50$ kPa. The compositions of propene (1) and propane (2) downstream of the membrane were not reported in Kapteijn et al. [4] and these were assumed to be negligibly small, i.e. $p_{1\delta}=0$ kPa; $p_{2\delta}=0$ kPa. The Fick matrix of diffusivities was calculated using Eq. (5).

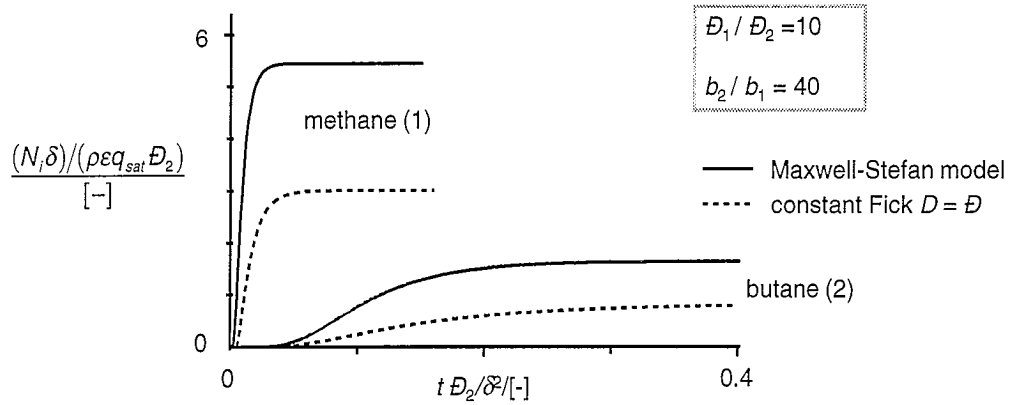

Fig. 7. Simulations for transport of individual components methane (1) and butane (2) across silicalite-1 membrane. The membrane thickness is $\delta=40$ mm. The temperature was maintained at 292 K. The parameter inputs are: $b_1=0.008$ kPa^{-1}; $b_2/b_1=40$; $Đ_1/Đ_2=10$. The upstream partial pressures of the methane (1) $p_{10}=50$ kPa; butane (2): $p_{20}=50$ kPa. The downstream pressure was maintainted at $p_\delta=50$ kPa and a sweep gas was used and the partial pressures of the permeating component methane was considered to be practically zero at the downstream side $p_{1\delta}=0$ kPa. The flux was calculated using (i) the single file diffusion model $D_1=Đ_1/(1-\theta_1)$ and (ii) a model in which the Fick diffusvity is taken to be constant and equal to $D_1=Đ_1$. The Maxwell–Stefan diffusivities and the Langmuir isotherm single component parameters were culled from Kapteijn et al. [4,10] and Bakker et al. [5].

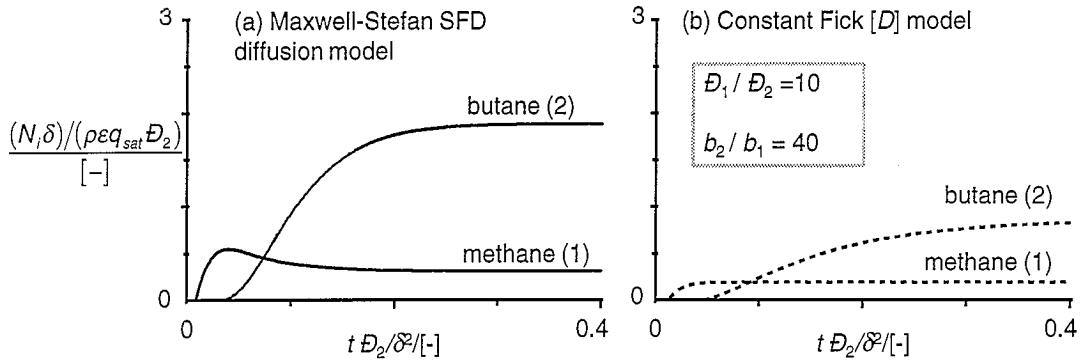

Fig. 8. Simulations for transport of methane (1)-*n*-butane (2) across silicalite-1 membrane. The membrane thickness is $\delta=40$ mm. The temperature was maintained at 292 K. The parameter inputs are: $b_1=0.008$ kPa^{-1}; $b_2/b_1=40$; $Đ_1/Đ_2=10$. The upstream partial pressures of the methane (1) and butane (2) are $p_{10}=50$ kPa; $p_{20}=50$ kPa. The downstream pressure was maintainted at $p_\delta=100$ kPa and a sweep gas was used and the partial pressures of the permeating components were considered to be practically zero at the downstream side $p_{1\delta}=0$ kPa; $p_{2\delta}=0$ kPa. The Fick matrix of diffusivities was calculated using both (a) the Maxwell–Stefan single-file diffusion (SFD) diffusion model (Eq. (5)), and (b) the constant Fick [D] model (Eq. (7)). The Maxwell–Stefan diffusivities and the Langmuir isotherm single component parameters were culled from Kapteijn et al. [4] and Bakker et al. [5].

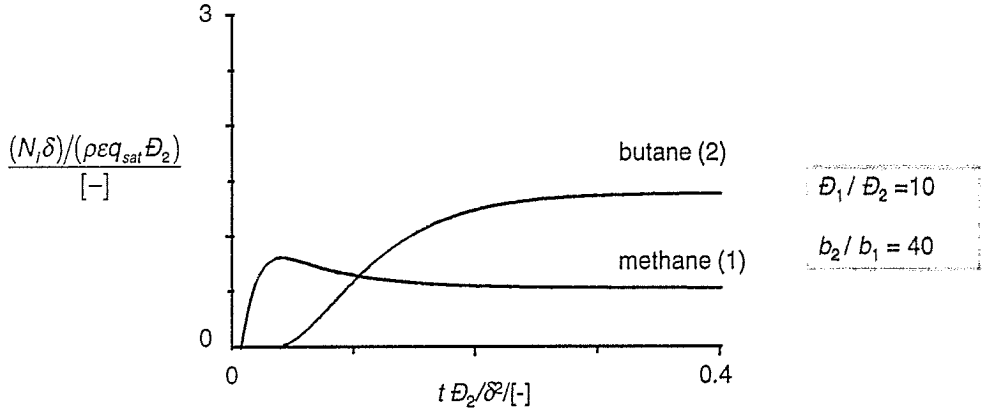

Fig. 9. Simulations for transport of methane (1)-*n*-butane (2) across silicalite-1 membrane. The membrane thickness is δ = 40 mm. The temperature was maintained at 292 K. The parameter inputs are: b_1 = 0.008 kPa^{-1}; b_2/b_1 = 40; $Đ_1/Đ_2$ = 10. The upstream partial pressures of the methane (1) and butane (2) are p_{10} = 95 kPa; p_{20} = 5 kPa. The downstream pressure was maintainted at p_δ = 100 kPa and a sweep gas was used and the partial pressures of the permeating components were considered to be practically zero at the downstream side $p_{1\delta}$ = 0 kPa; $p_{2\delta}$ = 0 kPa. The Fick matrix of diffusivities was calculated using both the Maxwell–Stefan single file diffusion (SFD) diffusion model (Eq. (5)). The Maxwell–Stefan diffusivities and the Langmuir isotherm single component parameters were culled from Kapteijn et al. [4] and Bakker et al. [5].

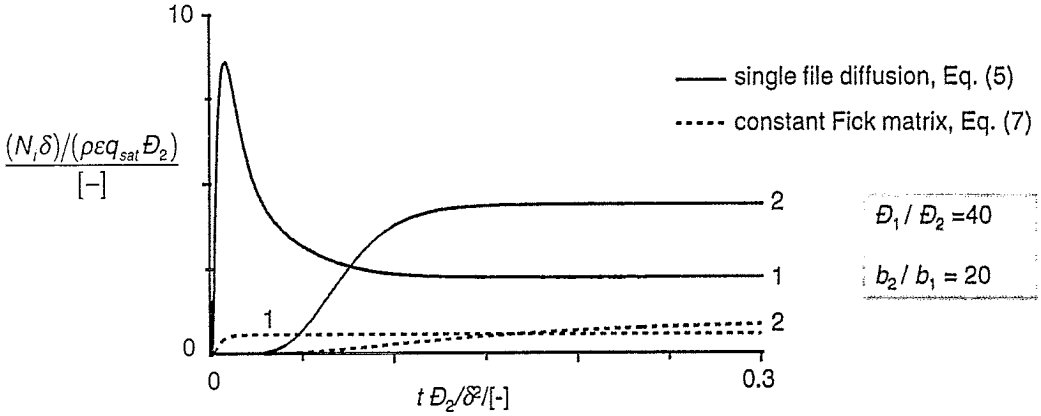

Figure 10. Simulations for transport of hydrogen (1)-*n*-butane (2) across silicalite membrane. The following parameter values were assumed. The parameter inputs are: b_1 = 0.1 kPa^{-1}; b_2/b_1 = 20; $Đ_1/Đ_2$ = 40; $p_{1\delta}$ = 0 kPa; $p_{2\delta}$ = 0 kPa. The Fick matrix of diffusivities was calculated using Eqs. (5) and (7).

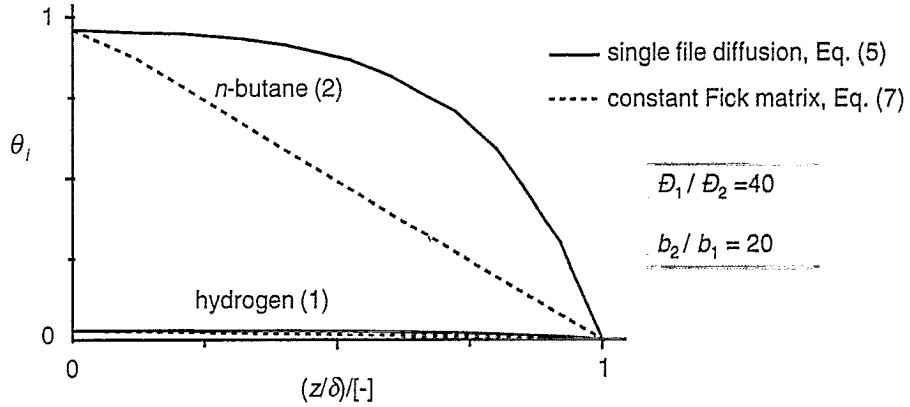

Fig. 11. The coverage profiles obtained for steady state conditions in the simulations of Fig. 6. The two profiles correspond to the micropore diffusion models given by Eqs. (5) and (7).

the permeation behaviour of a mixture of methane and *n*-butane for which the adsorption strengths and the Maxwell–Stefan diffusivities are significantly different; this system can be expected to provide a more stringent test of the permeation model used in the simulations.

3.2. Simulation of permeation experiments with methane (1) and n-butane (2)

Firstly, we simulated the single component permeation experiments portrayed in Fig. 4. For these simulations the necessary parameters for the diffusivities and adsorption strengths were culled from the papers of Kapteijn et al. [4,10]. In the experiments of Bakker et al. [5], it is seen that the partial pressures of the permeating components on the downstream side have small but finite values. For our simulations we assume these partial pressures to be vanishingly small. This assumption does not alter the main conclusions of this paper because the driving forces for diffusion are overestimated to only a small extent. The simulation results are shown in Fig. 7, here two different models have been used: (i) the Maxwell–Stefan model (Eq. (5)); and (ii) the constant Fick diffusivity model (Eq. (7)). The single permeation simulations show that the flux of methane is significantly higher than the flux of *n*-butane, as is observed experimentally; see Fig. 4(a). The constant Fick diffusivity model, assuming $D=Đ$ also predicts the same trends but the flux values are different.

For the 50:50 mixture of methane (1)/*n*-butane (2), the simulations with (i) the Maxwell–Stefan single file diffusion model with coverage independent $Đ_i$ (Eq. (5)) and (ii) the constant Fick diffusivity model (Eq. (7)) are seen to be qualitatively different; compare Figs. 8(a) and (b). The Maxwell–Stefan model predicts a maximum in the flux of methane before this flux reduces to low values. This maximum is in conformity with the experimental observation in Fig. 4(b). The constant Fick diffusivity model predicts a monotonic approach to steady state, not in conformity with the experiments. These results provide a strong support of the Maxwell–Stefan formulation. For the binary permeation simulations presented in Fig. 8 we used the extended Langmuir isotherm, Eq. (2), for calculating the multicomponent equilibrium. Accurate multicomponent equilibrium will be required for quantitative simulations.

The reasoning behind the maximum permeation flux of methane is as follows. Initially we begin with completely uncovered, membrane pore walls. The initial permeation fluxes will be dictated by differences in the mobilities (diffusivities) of the components inside the pores. Methane has a higher diffusivity and its initial flux is higher. The adsorbed methane molecular species will (slowly) become displaced by the more strongly adsorbed *n*-butane. Higher adsorption leads to higher occupancy and a higher driving force for diffusion. The permeation flux of *n*-butane will tend to rise at the expense of methane (the adsorbed methane within the pores will be replaced by *n*-butane). This leads to a decline in the flux of methane and an increase in the flux of *n*-butane.

Another feature of the Maxwell–Stefan formulation is that the occupancies of the species influence the overall transfer rates, higher occupancies will lead to higher Fick diffusivities (cf. Eq. (5)). Increasing the feed composition of a particular component will have the effect of increasing the occupancy of this particular component and therefore will enhance its flux. In Fig. 9 we present the simulation of the experiments with methane (1) and *n*-butane (2) in which $p_{10}=95$ kPa, $p_{20}=5$ kPa. With the Maxwell–Stefan diffusion model we note that the maximum flux of methane is increased beyond the value observed in Fig. 8, which again is in conformity with the experimental results of Fig. 4(c). We conclude that the Maxwell–Stefan equation is also able to predict the right trend with varying feed compositions.

3.3. Simulation of permeation experiments with hydrogen (1) and n-butane (2)

The Maxwell–Stefan diffusivity data for hydrogen permeation in the zeolite membrane is not available, but we can expect it to be higher than that for methane. In the simulations shown in Fig. 10 we have assumed $Đ_1/Đ_2=40$. This choice leads to very high initial flux of hydrogen, a factor five or so higher than the steady-state flux. This trend has been observed in the experiments of Bakker [3] (cf. Fig. 2). The constant Fick [D] model predicts a monotonic approach to steady-state, not in conformity with experimental results. A proper description of the multicomponent equilibrium will be required for quantitative simulations but a comparison of Figs. 2 and 10 shows the potency of the Maxwell–Stefan formulation.

For the steady-state situation in Fig. 10, the occupancies of the components hydrogen (1) and *n*-butane (2) are shown in Fig. 11 for the Maxwell–Stefan and the constant Fick [D] models. The coverage profiles are significantly different.

4. Conclusions

By simulations of the transient permeation fluxes of binary mixtures of hydrocarbons we have demonstrated conclusively that the Maxwell–Stefan formulation is able to explain correctly the qualitative trends. Especially interesting are the experiments with methane/*n*-butane and hydrogen/*n*-butane where the curious phenomenon of flux maximum of the faster diffusing species is observed. This phenomenon can be modelled by the Maxwell–Stefan approach and not by the simple Fick model.

We conclude that the Maxwell–Stefan formulation is indispensable in the description of transport across zeolite membranes.

References

[1] J.A. Wesselingh and R. Krishna, *Mass Transfer*, Ellis Horwood, Chichester, 1990.

[2] M.B. Rao and S. Sircar, Nanoporous carbon membrane for gas separation, *Gas Sep. Purif., 7* (1993) 279–284.

[3] W.J.W. Bakker, Metal supported zeolite membranes for separation processes, in A.C.M. Franken (ed.), *OSPT Procestechnologie*, 1993, p. 65.

[4] F. Kapteijn, W.J.W. Bakker, G. Zheng, J. Poppe and J.A. Moulijn, Permeation and separation of light hydrocarbons through a silacalite-1 membrane. Application of the generalized Maxwell–Stefan equations, *Chem. Eng. J., 57* (1995) 145–153.

[5] W.J.W. Bakker, G. Zheng, F. Kapteijn, M. Makkee and J.A. Moulijn, Single and multi-component transport through metal-supported MFI zeolite membranes, in M.P.C. Weijnen and A.A.H. Drinkenburg (eds.), *Precision Process Technology*, Kluwer, Netherlands, 1993, pp. 425–436.

[6] R. Krishna, Multicomponent surface diffusion of adsorbed species: a description based on the generalized Maxwell–Stefan equations, *Chem. Eng. Sci., 45* (1990) 1779–1791.

[7] R. Krishna, Problems and pitfalls in the use of the Fick formulation for intraparticle diffusion, *Chem. Eng. Sci., 48* (1993) 845–861.

[8] R. Krishna, A unified approach to the modelling of intraparticle diffusion in adsorption processes, *Gas Sep. Purif., 7* (1993) 91–104.

[9] W.E. Schiesser, *The numerical method of lines: integration of partial differential equations*, Academic Press, San Diego, CA, 1991.

[10] F. Kapteijn, W.J.W. Bakker, G. Zheng, J. Poppe and J.A. Moulijn, The temperature and occupancy dependent diffusion on *n*-butane through a silicalite membrane, *Micropor. Mater.*, in press.

Appendix A: Nomenclature

b_i parameter in the Langmuir adsorption isotherm, kPa^{-1} or Pa^{-1}

D Fick diffusivity of single component in membrane, m^2s^{-1}

$[D]$ matrix of Fick diffusivities for multicomponent system, m^2s^{-1}

$Đ_i$ Maxwell–Stefan diffusivity of component i, m^2s^{-1}

$Đ_{ref}$ reference value of Maxwell–Stefan diffusivity, m^2s^{-1}

Fo Fourier number, $Đ_{ref}\, t/\delta^2$

N_i molar flux of species i, mol $m^{-2}s^{-1}$

p_i partial pressure of species i, Pa

q_i adsorbed species concentration within micropores, mol kg^{-1}

q_{sat} total saturation concentration, mol kg^{-1}

R gas constant, 8.314 J $mol^{-1}K^{-1}$

t time, s

T absolute temperature, K

z direction coordinate, m

Greek letters

$[\Gamma]$ matrix of thermodynamic factors

δ thickness of membrane, m

δ_{ij} Kronecker delta

ϵ porosity of membrane

θ_i fractional surface occupancy of component i

$\theta_{i,sat}$ fractional surface occupancy of component i at saturation

θ_V fraction unoccupied sites

η dimensionless distance along membrane

ρ density of membrane, kg m^{-3}

Subscripts

i referring to component i

sat parameter value at saturation

δ referring to position $z = \delta$

0 referring to position $z = 0$

Superscript

* equilibrium value